

Selecting the best growth model for elasmobranches

Age and growth information is essential for accurate stock assessment of fish, and growth model selection may influence the result of stock assessment. Previous descriptions of the age and growth of elasmobranches relied mainly on the von Bertalanffy growth model (VBGM). However, it has been noted that sharks, skates and rays exhibit significant variety in size, shape, and life-history traits. Given this variation, the VBGM may not necessarily provide the best fit for all elasmobranches. This study attempts to improve the accuracy of age estimates by testing four growth models—the VBGM, two-parameter VBGM, Robertson (Logistic) and Gompertz models—to fit observed and simulated length-at-age data for 37 species of elasmobranches. The best growth model was selected based on corrected Akaike's Information Criterion (AIC_c), the AIC_c difference, and the AIC_c weight. The VBGM and two-parameter VBGM provide the best fit for species with slow growth and extended longevity ($L_\infty > 100$ cm TL, $0.05 < k < 0.15$ yr⁻¹), such as pelagic sharks. For fast-growing small sharks ($L_\infty < 100$ cm TL, k_r or $k_g > 0.2$ yr⁻¹) in deep waters and for small-sized demersal skates/rays, the Robertson and the Gompertz models provide the best fit. The best growth models for small sharks in shallow waters are the two-parameter VBGM and the Robertson model, while all the species best fit by the Gompertz model are skates and rays.

1 **Selecting the best growth model for elasmobranches**

2 Kwang-Ming Liu^{1,2,3*}, Chiao-Bin Wu¹, Shoou-Jeng Joung^{3,4}, and Wen-Pei Tsai⁵

3

4 ¹ Institute of Marine Affairs and Resource Management, National Taiwan Ocean
5 University, 2 Pei-Ning Road, Keelung 20224, Taiwan.

6 ² George Chen Shark Research Center, National Taiwan Ocean University, 2 Pei-
7 Ning Road, Keelung 20224, Taiwan.

8 ³Center of Excellence for the Oceans, National Taiwan Ocean University, 2 Pei-Ning
9 Road, Keelung 20224, Taiwan.

10 ⁴Department of Environmental Biology and Fisheries Science, National Taiwan
11 Ocean University, 2 Pei-Ning Road, Keelung 20224, Taiwan.

12 ⁵Department of Fishery Production and Management, National Kaohsiung Marine
13 University, 2 Haitzuan Road, Kaohsiung 811, Taiwan

14 *: corresponding author

15 E-mail: kmliu@mail.ntou.edu.tw

16 Tel: +886-2-24622192 ext. 5018. Fax: +886-2-24620291

17

18

19 **ABSTRACT**

20 Age and growth information is essential for accurate stock assessment of fish, and
21 growth model selection may influence the result of stock assessment. Previous
22 descriptions of the age and growth of elasmobranchs relied mainly on the von
23 Bertalanffy growth model (VBGM). However, it has been noted that sharks, skates
24 and rays exhibit significant variety in size, shape, and life-history traits. Given this
25 variation, the VBGM may not necessarily provide the best fit for all elasmobranchs.
26 This study attempts to improve the accuracy of age estimates by testing four growth
27 models—the VBGM, two-parameter VBGM, Robertson (Logistic) and Gompertz
28 models—to fit observed and simulated length-at-age data for 37 species of
29 elasmobranchs. The best growth model was selected based on corrected Akaike's
30 Information Criterion (AIC_c), the AIC_c difference, and the AIC_c weight. The VBGM
31 and two-parameter VBGM provide the best fit for species with slow growth and
32 extended longevity ($L_\infty > 100$ cm TL, $0.05 < k < 0.15$ yr⁻¹), such as pelagic sharks.
33 For fast-growing small sharks ($L_\infty < 100$ cm TL, k_r or $k_g > 0.2$ yr⁻¹) in deep waters
34 and for small-sized demersal skates/rays, the Robertson and the Gompertz models
35 provide the best fit. The best growth models for small sharks in shallow waters are
36 the two-parameter VBGM and the Robertson model, while all the species best fit by
37 the Gompertz model are skates and rays.

38

39 **INTRODUCTION**

40 Most elasmobranches are characterized by a K-selection life history; slow growth,
41 late maturation, extended longevity, few offspring, and low mortality (Hoenig &
42 Gruber, 1990; King & McFarlane, 2003; Winemiller & Rose, 1992). Elasmobranches
43 also take a long time to recover when subjected to high fishing pressure. Three
44 reproductive strategies, oviparity, viviparity, and aplacental viviparity, have been
45 identified for elasmobranches, and a variety of external morphologies, sizes, and life
46 histories have been found. In short, the life history traits, particularly the reproductive
47 traits of elasmobranches, are more complex than those of teleosts, which are mostly
48 oviparous.

49

50 Similar to many marine mammals, elasmobranches are among the ocean's top
51 predators, and their life history characteristics make them vulnerable to
52 overexploitation. A collapse of the elasmobranch population could result in
53 imbalances in marine ecosystems (Stevens et al., 2000). Age, growth, and
54 reproduction parameters are crucial for accurate stock assessment and evaluation of
55 their population dynamics (Cailliet et al., 1986, Cailliet & Goldman, 2004).
56 Information on age and growth can be used in natural mortality, longevity, and yield-
57 per-recruit estimates (Ismen, 2003). In the 1950s, Beverton & Holt (1957) first
58 applied the von Bertalanffy growth model (VBGM) to fish population dynamics.
59 However, VBGM may not necessarily provide the best fit for all elasmobranches
60 (Cailliet & Goldman, 2004). Therefore, selecting the most appropriate growth model
61 is important in stock assessment and fishery management of elasmobranches
62 (Gelsleichter et al., 1998).

63

64 Four growth models are commonly used in description of age and growth of
65 elasmobranchs: the VBGM, the two-parameter VBGM, the Robertson (Logistic)
66 model, and the Gompertz model (Cailliet et al., 2006). Numerous examples exist that
67 used VBGM to estimate the age and growth of elasmobranchs. These include studies
68 on the bonnethead shark *Sphyrna tiburo* (Carlson & Parsons, 1997), smalltail shark
69 *Carcharhinus porosus* (Lessa & Santana, 1998), pelagic thresher *Alopias pelagicus*
70 (Liu et al., 1999), whiskery shark *Furgaleus macki* (Simpfendorfer et al., 2000),
71 undulate ray *Raja undulate* (Coelho & Erzini, 2002), Atlantic sharpnose shark
72 *Rhizoprionodon terraenovae* (Carlson & Baremore, 2003), winter skate *Leucoraja*
73 *ocellata* (Sulikowski et al., 2003), thorny skate *Amblyraja radiata* (Sulikowski et al.,
74 2005), yellownose skate *Dipturus chilensis* (Licandeo et al., 2006), common
75 guitarfish *Rhinobatos rhinobatos* (Ismen et al., 2007), and deepwater lantern shark
76 *Etmopterus spinax* (Coelho & Erzini, 2008).

77

78 Although the VBGM is the most commonly-used growth model, others have also
79 been employed. The two-parameter VBGM has been successfully applied in
80 describing growth of the bull shark *Carcharhinus leucas* (Neer et al., 2005) and the
81 female shortfin mako shark *Isurus oxyrinchus* (Chang & Liu, 2009; Semba et al.,
82 2009), for which size-at-birth data are available. An S-sharp model (Gompertz model)
83 has been used to estimate the growth of the Pacific electric ray *Torpedo californica*
84 (Neer & Cailliet, 2001), pelagic stingray *Dasyatis violacea* (Mollet et al., 2002) and
85 Alaska skate *Bathyraja parmifera* (Matta & Gunderson, 2007), while the Robertson
86 (Logistic) model has been used to fit the size-at-age data for the spinner shark
87 *Carcharhinus brevipinna* (Carlson & Baremore, 2005) and the dusky shark
88 *Carcharhinus obscurus* (Natanson et al., 2014; Joung et al., 2015).

89

90 In some cases, particularly in recent years, a variety of models have been used in age
91 and growth studies of sharks. These include studies on the tiger shark *Galeocerdo*
92 *cuvier* (Kneebon et al., 2008; Wintner & Dudley, 2000), bull shark *C. leucas* (Wintner
93 et al., 2002), blue shark *Prionace glauca* (Lessa et al., 2004), sandbar shark *C.*
94 *plumbeus* (Romine et al., 2006), shortfin mako (Natanson et al., 2006), whitespotted
95 bamboo shark *Chiloscyllium plagiosum* (Chen et al., 2007), smooth skate *Malacoraja*
96 *sentia* (Natanson et al., 2007), scalloped hammerhead *S. lewini* (Piercy et al., 2007),
97 sharpnose skate *Okameieia acutispina* (Joung et al., 2011), dusky shark
98 (Simpfendorfer et al., 2002; Natanson et al., 2014; Joung et al., 2015), and spinner
99 shark (Geraghty et al., 2014). The use of different models in fitting length-at-age data
100 is considered preferable. Araya & Cubillos (2006) stated that a two-phase growth
101 model provides a better estimate of elasmobranch growth than the VBGM. This
102 finding was later supported by Braccini et al. (2007) in their study of the piked
103 spurdog *Squalus megalops*.

104

105 Chen (pers. comm., 2004) applied several growth models to a variety of teleost
106 species and concluded that the Richards and Robertson models best fit fish with
107 slender and long lateral profiles, while the VBGM and Gompertz model best fit other
108 species. Romney & Campana (2009) examined four skate species and concluded that
109 the VBGM best fit the winter and thorny skate *Amblyraja radiata*, while the
110 Robertson model best fit the little skate, *Raja erinaceian*, and the Gompertz model
111 best fit the smooth skate. Ebert et al. (2007) concluded that the VBGM provided the
112 best fit for the Aleutian skate *Bathyraja aleutica* but that the Bering skate *B.*
113 *interrupta* was more accurately described by the Robertson model. Katsanevakis

114 (2006) also concluded that different growth models best described the growth of
115 different chondrichthyan fish.

116

117 Given the influence of growth model selection on the results of stock assessment, in
118 particular, age-structured models, the objectives of this study were twofold: first, to fit
119 the length-at-age data using different growth models, selecting the best model for
120 each species; and second, to group species on the basis of the best-fit model, examine
121 the life history traits for each of these groups, and discuss the possible factors
122 involved. We hope that our findings can provide an important future reference for the
123 selection of the most appropriate growth model for elasmobranches.

124

125 **MATERIALS AND METHODS**

126 **Source of data**

127 This study collected and analyzed the length-at-age data of 37 species, including the
128 observations of vertebral band counts of 7 species in Taiwanese waters and the age-
129 length key data of 30 species from the literature (Table 1). These species fell into 6
130 orders and 12 families (Table 2). Two species were from Hemiscylliidae and
131 Rhincodontidae (Orectolobiformes), 2 were from Odontaspidae, and Alopiidae
132 (Lamniformes), 19 were from Triakidae, Carcharhinidae, and Sphyrnidae
133 (Carcharhiniformes), 2 were from Etmopteridae (Squaliformes), 11 were from
134 Rhinobatidae and Rajiformes (Rajidae), and 1 was from Dasyatidae
135 (Myliobatiformes). Life history parameters and ecological information, including
136 habitat information, reproductive strategy, fecundity, reproductive cycle (R_c), and size
137 at maturity (L_{mat}), were collected through literature searches in FishBase
138 (<http://www.fishbase.net/>) as well as from published scientific articles and gray

139 literature.

140

141 **Data process**

142 In addition to observed length-at-age data, age-length key data adopted from the

143 literature comprised the following data sets: (1) detailed age-specific length

144 distribution data that can be directly fitted by the growth models, (2) age-specific

145 mean length with standard deviation, and (3) age-specific length interval. For data

146 sets 2 and 3, a simulation process was used to generate (mimic) individual

147 observations. For data set 2, a normal random number generator was used to generate

148 100 sets of observations based on the sample size, mean length, and standard

149 deviation for each age. The simulated data set was adopted when its mean length and

150 standard deviation were equal to the observed values. For data set 3, the length

151 distribution of each age was assumed to be a uniform distribution, and a total of 100

152 sets of observations were generated from a uniform random number generator based

153 on the sample size and the maximum and minimum length of each age. The simulated

154 data set was adopted when its mean length (the average of the maximum and the

155 minimum length) was equal to the observed value.

156

157 The literature reveals an inconsistency in the way that body length is measured. Total

158 length (TL) of 26 species, fork length (FL) of 3 species, precaudal length (PCL) of 7

159 species, and disc width (DW) of 1 species have all been used. Size-at-birth data were

160 available for 21 of the 37 species (Table 1). Our analysis converted all length data to

161 TL using linear relationships between TL and other measurements.

162

163 **Data analysis**

164 Growth models

165 Three commonly used growth models, the VBGM (von Bertalanffy, 1938), the
166 Robertson (Logistic) (Robertson, 1923) and the Gompertz (Gompertz, 1825), were
167 fitted to the length-at-age data for all species. For those species where size-at-birth
168 data were available, an additional model, the two-parameter VBGM (Fabens, 1965),
169 was also used. The NLIN procedure of the statistical package SAS ver. 9.0 (SAS
170 Institute, 2008, Cary, NC, USA) was used to estimate the parameters of each model.
171 The four growth models are described as follows:

172 (1) VBGM (von Bertalanffy, 1938)

$$173 L_t = L_\infty (1 - \exp(-k(t - t_0)))$$

174 (2) Two-parameter VBGM (Fabens, 1965)

$$175 L_t = L_\infty (1 - ((L_\infty - L_0) \exp(-kt)) / L_\infty)$$

176 (3) Robertson (Logistic) model (Robertson, 1923)

$$177 L_t = L_\infty (1 + \exp(c_r - k_r t))^{-1}$$

178 (4) Gompertz model (Gompertz, 1825)

$$179 L_t = L_\infty \exp(-c_g \times \exp(-k_g t))$$

180 where L_t is the length at age t , L_∞ is the asymptotic length, k is the growth coefficient,
181 t is the age (year from birth), t_0 is the age at length 0, c_r and k_r are the parameters of
182 the Robertson model, and c_g and k_g are the parameters of the Gompertz model.

183

184 Model selection

185 The goodness of fit of the four growth models was compared based on the corrected
186 Akaike's Information Criterion (AIC_c), the AIC_c difference (ΔAIC_c), and the AIC_c
187 weight (w_i) (Burnham & Anderson 2002). AIC_c was expressed as:

$$188 \quad AIC_c = AIC + \frac{2K(K+1)}{n-K-1},$$

$$189 \quad AIC = n \times \ln(MSE) + 2K \quad (\text{Akaike 1973}),$$

190 where n is the total sample size, MSE is the mean square of residuals, and K is the
191 number of parameters estimated in the growth model. The AIC_c difference (ΔAIC_c) of
192 each model was calculated as the difference between $AIC_{c,i}$ and the lowest observed
193 AIC_c value (AIC_{cmin}). Models with ΔAIC_c less than 2 have good support, while those
194 with greater than 10 have no support. The corrected Akaike weight (W_i) is expressed
195 as a percentage, which is useful when there are only minor differences in AIC_c values
196 among the growth models (Burnham & Anderson 2002). AIC_c weights with higher
197 values (indicating a better fit) can be expressed as follows:

$$198 \quad W_i = \frac{\exp(-0.5\Delta_i)}{\sum_{m=1}^4 \exp(-0.5\Delta_m)},$$

199 where m is the number of growth models being analyzed.

200

201 **RESULTS**

202 **VBGM as the best growth model**

203 The VBGM provided the best fit for 4 shark species: the pelagic thresher, blue shark,
204 night shark *Carcharhinus signatus*, and tiger shark; and 2 skates: roundel skate, and
205 blue skate *R. batis* (Table 3). All are large-size sharks or skates except the roundel
206 skate and blue skate. The tiger shark had the highest L_∞ ($L_\infty = 364.3$ cm TL), while the
207 blue skate had the lowest ($L_\infty = 47.6$ cm TL). The blue skate had the slowest growth
208 rate ($k = 0.024$ yr⁻¹), while the roundel skate had the fastest ($k = 0.194$ yr⁻¹).

209

210 **Two-parameter VBGM as the best growth model**

211 The two-parameter VBGM provided the best fit for 16 species, of which 13 were
212 sharks and 3 were skates/rays, comprising 52% and 25% of the 25 species of sharks
213 and 12 species of skates/rays, respectively (Fig. 1).

214

215 Only the smooth lantern shark, the Atlantic sharpnose shark, and the cuckoo ray *R.*
216 *naevus* had an $L_{\infty} < 100$ cm TL. The remaining species had an $L_{\infty} > 100$ cm TL. The
217 silky shark had the highest L_{∞} ($L_{\infty} = 315.2$ cm TL), while the smooth lantern shark
218 had the lowest ($L_{\infty} = 53.1$ cm TL). The Atlantic sharpnose shark had the fastest
219 growth rate ($k = 0.582$ yr⁻¹), while the gummy shark had the slowest ($k = 0.072$ yr⁻¹).
220 The exceptionally large-sized whale shark also fell into this group, with $L_{\infty} = 1580$ cm
221 TL and $k = 0.020$ yr⁻¹ (Table 4).

222

223 **Robertson model as the best growth model**

224 The Roberson model provided the best fit for 12 species (Table 5), including 8 sharks
225 and 4 skates/rays, comprising 32% and 33% (Fig. 1) of the sharks and skates/rays in
226 this study, respectively. Five species (42%) were large sharks, 3 species (25%) were
227 small sharks, and 4 species (33%) were skates/rays (Fig. 2).

228

229 The thorny skate, blacknose shark *Carcharhinus acronotus*, spinner shark, daggernose
230 shark *Isogomphodon oxyrinchus*, school shark *Galeorhinus galeus*, and dusky shark
231 fell into the large-size category ($L_{\infty} > 100$ cm). The remainder fell into the small-size
232 category ($L_{\infty} < 100$ cm). The dusky shark had the largest L_{∞} ($L_{\infty} = 362.9$ cm), while
233 the deepwater lantern shark had the smallest ($L_{\infty} = 42.3$ cm). The little skate had the
234 fastest growth rate ($k_r = 0.665$ yr⁻¹), while the dusky shark had the slowest ($k_r = 0.131$
235 yr⁻¹).

236

237 **Gompertz model as the best growth model**

238 The Gompertz model (Table 6) provided the best fit for three species, including
239 yellownose skate, winter skate, and Kwangtung skate *Dipturus kwangtungensis* (Fig.
240 1).. One species was a small skate (33%), and 2 species (67%) were large skates (Fig.
241 2).

242

243 The Kwangtung skate fell into the small-size category ($L_{\infty} < 100$ cm). While the
244 yellownose skate and winter skate fell into the large-size category ($L_{\infty} > 100$ cm). as
245 The yellownose skate had the fastest growth rate ($k_g = 0.192 \text{ yr}^{-1}$), while the
246 Kwangtung skate had the slowest ($k_g = 0.114 \text{ yr}^{-1}$).

247

248 In summary, sharks were best fitted by the two-parameter VBGM (52%), while
249 skates/rays were best fitted by the Robertson model (33%). Large sharks were best
250 fitted by the two-parameter VBGM (44%), small sharks were best fitted by the
251 Robertson model (60%), and skates/rays were best fitted by the Robertson model
252 (33%) (Fig. 3). The species best fitted by the Gompertz model were all skates and
253 rays (100%).

254

255 **DISCUSSION**

256 Cailliet & Goldman (2004) intensively reviewed 115 publications on the age and
257 growth of 91 species of chondrichthyans, and Cailliet et al. (2006) presented updated
258 information on 28 new studies. However, most of these studies did not provide either
259 length-at-age or age-length key data. Thus, only 37 species with either observed
260 length-at-age or age-length key data were used in this study.

261

262 Uncertainties

263 As mentioned above, observed length-at-age data were available for only 7 of 37
264 species. For the remaining 30 species, figures were generated (simulated) from age-
265 length key data. Because such simulations may not be representative of real
266 observations, there may be inaccuracies in the growth parameter estimates. Some
267 species were represented by a small sample size - the common stingray, sand tiger
268 shark, cuckoo skate, etc. Because of this, and due to a lack of small or large specimens,
269 the size-at-age data may not cover the whole life history of the fish. As a result,
270 estimated parameters might not accurately describe the growth over the entire life
271 history. Cailliet & Goldman (2004) stated that growth parameter estimates are greatly
272 influenced by a lack of very young or old individuals. The existence of length-at-birth
273 information may therefore have a significant effect on the choice of growth model. In
274 this study, the simulated observation data set was adopted only when its mean length
275 and standard deviation were equal to observed values. Several simulations were made
276 for each species and although minor variations in growth parameter estimates were
277 noted, this had no effect on the selection of best-fit growth model.

278

279 The basic theory of growth equation

280 Derived from the allometric relationship between metabolic rate and body weight, the
281 VBGM has been widely used to describe the growth of fish (Haddon, 2001). The
282 ideas underpinning this model are that energy transformation during growth can be
283 expressed as the difference between anabolism and catabolism and that the growth
284 rate decreases exponentially with age (Pütter, 1920). Beverton & Holt (1957) were the
285 first to apply the VBGM to the study of fisheries. The Gompertz model was originally

286 developed to estimate human mortality rates (Gompertz, 1825), while the Robertson
287 model was based on the logistic model used to describe population dynamics and
288 individual growth over time. Both models are S-shaped curves with inflection points
289 occurring at an intermediate age when the growth rate starts to decrease (Wang &
290 Zuidhof, 2004). The inflection point of the Robertson model occurs at 50% of L_{∞} , but
291 it occurs at approximately 37% of L_{∞} for the Gompertz model (Winsor, 1932). Under
292 these two models, growth rates increase with age to a maximum at the inflection
293 points and then decrease thereafter (Ricker, 1975, 1979). Discrepancies in life history
294 among elasmobranch species are likely to affect the result of selecting the best-fit
295 growth model.

296

297 Energy allocation in animals can be expressed as $C = R + G + S + W$, where C is
298 energy consumption, R is the catabolic rate, G is growth, S is spawning, and W is
299 waste (Winberg, 1960). Catabolism includes both standard and active forms (e.g.,
300 energy consumption when feeding). When more energy is allocated to reproduction
301 and growth, less can be allocated to catabolism and waste, and vice versa. Energy
302 allocation for elasmobranches varies with habitat and reproductive strategies; this may
303 result in differences in growth.

304

305 In this study, growth of the bull shark was best described by the two-parameter
306 VBGM. According to Schmid & Murru (1994), the juvenile bull shark allocates most
307 of its energy to catabolism and waste and little to growth. Conversely, the chain
308 dogfish *Scyliorhinus rotifer*, the growth of which was best described by the Robertson
309 model in this study, allocates most of its energy to growth and reproduction (Duffy,
310 1999). This suggests that small-size species allocate the most energy to growth and

311 reproduction, while the converse is true for large-size species. The fact that the
312 VBGM or two-parameter VBGM best fit large sharks, while the Robertson and
313 Gompertz models best fit small sharks may therefore be related to their energy
314 allocation.

315

316 Cailliet & Goldman (2004) suggested that the Gompertz model better describes
317 changes in body weight over time than changes in length. However, this hypothesis
318 cannot be tested because age-at-weight data are not available in the literature. Most
319 sharks are torpedo-shaped and large, while most skates and rays are flat and small.
320 The best growth model might be related to the ratio of size-at-maturity and maximum
321 observed size. Species for which the VBGM and two-parameter VBGM provide the
322 best fit are mostly sharks that tend to be late-maturing (Table 7), e.g., the pelagic
323 thresher shark, bull shark and blacktip shark. Species best fitted by the Robertson and
324 Gompertz models tend, in contrast, to be early-maturing, such as the common stingray,
325 sharpnose skate, and blue skate (Table 7).

326

327 **Other growth models**

328 The four-parameter Richards growth model is a general form of the VBGM,
329 Robertson, and Gompertz models and is considered superior to the three-parameter
330 growth models (Quinn & Deriso, 1999). However, in this study, the lack of large
331 specimens and the relatively small sample size for certain species may cause the
332 inconvergence of iterations in parameter estimation by non-linear procedures. Araya
333 & Cubillos (2006) used a two-phase growth model (TPGM) to fit for the porbeagle
334 shark *Lamna nasus* and leopard shark *Triakis semifasciata*. The TPGM is a five-
335 parameter growth model; the additional parameter is the age at which transition

336 between two phases occurs. Because more detailed age-length data are required for
337 this model, it was not applied in this study.

338

339 **Estimation of parameters**

340 In this study, L_{∞} estimates derived by the VBGM and two-parameter VBGM models
341 were larger than those derived by the Robertson and Gompertz models (Fig. 4). A
342 similar finding has been documented by Katsanevakis & Maravelias (2008). Therefore,
343 it seems that L_{∞} is closely related to growth model selection.

344

345 In this study, the VBGM provided the best fit for 6 species, with estimated k values of
346 $0.024 - 0.194 \text{ year}^{-1}$. All of these are moderate or slow-growing species ($k < 0.2 \text{ year}^{-1}$).

347 The two-parameter VBGM model was the best fit for 16 species, with estimated k
348 values of $0.020 - 0.582 \text{ year}^{-1}$. Most of these are also moderate- or slow-growing
349 species ($k < 0.2 \text{ year}^{-1}$), the exceptions being the Atlantic sharpnose shark

350 *Rhizoprionodon terraenovae*, finetooth shark *Carcharhinus isodon*, blacktip shark *C.*

351 *limbatus*, and common guitarfish *Rhinobatos* ($k > 0.2 \text{ year}^{-1}$). The Robertson model

352 provided the best fit for 12 species, with estimated k_r values of $0.131-0.667 \text{ year}^{-1}$.

353 Most of these are fast-growing species ($k_r > 0.2 \text{ year}^{-1}$), the exception being the dusky

354 shark ($k_r < 0.2 \text{ year}^{-1}$). The Gompertz model was the best fit for 3 species, with

355 estimated k_g values of $0.1138-0.1915 \text{ year}^{-1}$. These included moderate-growing

356 species, the yellownose skate, winter skate, and Kwangtung skate ($0.1 < k_g < 0.2 \text{ year}^{-1}$).

357 The VBGM and two-parameter VBGM provided the best fit for slow-to moderate-

358 growing species, while the Gompertz model was the best fit for moderate-growing

359 species, and the Robertson model was the best fit for fast-growing species.

360

361 Contingency of fitting models

362 For the 6 species best fitted by the VBGM, the second-best choice was the Gompertz
363 (100%) (Fig. 5). For the two-parameter VBGM (16 species), the second-best choice
364 was VBGM (81%), while for the Robertson (12 species), the second-best choice was
365 the Gompertz (100%). For the Gompertz model (3 species), the second-best choice
366 was the Robertson (67%). In short, the two-parameter VBGM best fits sharks, while
367 the Gompertz model best fits skates and rays. In their study of elasmobranches,
368 Katsanevakis & Maravelias (2008) proposed four growth models in order of fit, as
369 follows: Logistic-Gompertz-VBGM-Power (where Gompertz is the best choice, and
370 Logistic and VBGM are the second-best choices). They concluded that the VBGM
371 provided the best description of growth among elasmobranches and bony fish. Our
372 study arrived at a similar order of growth models, namely Robertson-Gompertz-
373 VBGM-two-parameter VBGM, although it should be noted that the previous study
374 separated species into sharks, skates, and rays. Mollet et al. (2002) found that the best
375 fit for the growth of the pelagic stingray was the Gompertz model. In this study, the
376 growth of skates/rays is best described by the S-shaped Gompertz or Robertson
377 models.

378

379 Comparison with literature results

380 Of the 37 species analyzed in this study, 12 have been previously fitted with more
381 than one growth model in the literature. Of these, our study found the same best
382 growth model for 10 species. The remaining 25 species have previously been
383 described using VBGM alone, but our study found that 19 of these species are better
384 fit by an alternative model. Thorson & Simpfendorfer (2009) have suggested using
385 AIC, AIC weight, and multi-model inference to obtain the most appropriate model to

386 describe fish growth. In this study, the best growth model for each stock was selected
387 based on similar criteria, AIC_c , ΔAIC_c , and the AIC_c weight, suggesting that the
388 derived results are reasonable.

389

390 **The relationship between life history traits and best growth model**

391 Based on their life history traits, three groups of sharks have been identified using
392 cluster analysis (Liu et al., 2015) as follows. Group 1: large size, extended life span,
393 slow growth, e.g., the silky shark, sandbar shark, scalloped hammerhead shark, and
394 oceanic whitetip shark. These are similar to the species best described in this study by
395 the two-parameter VBGM. Group 2: small size, short life span, rapid growth, e.g., the
396 smooth dogfish and blacknose shark. These are similar to the species best described in
397 this study by the Robertson model. Group 3: late-maturing, moderate life span, e.g.,
398 the pelagic thresher shark, tiger shark, blue shark and night shark. These are similar to
399 the species best described in this study by the VBGM. This study found that the
400 Robertson and Gompertz models provided the best fit for skates and rays. Those best
401 described by the Robertson model are characterized by small size and rapid growth,
402 e.g., the thorny skate, common stingray and little skate. Those best described by
403 Gompertz have the characters of small or large size and moderate growth, e.g., the
404 winter skate, yellownose skate, and Kwangtung skate.

405

406 As mentioned above, the Orectolobiformes, Lamniformes and large-sized species of
407 Carcharhidae are best fitted by the VBGM or two-parameter VBGM. Rajiformes
408 and Myliobatiformes are best fitted by the Robertson or Gompertz model, while the
409 Robertson model best describes the growth of small-size species of Carcharhidae.

410

411 Most species for which the VBGM or two-parameter VBGM provided the best fit are
412 viviparous, while most species best described by the Robertson or Gompertz models
413 are oviparous (Fig. 6). Species best described by the VBGM or two-parameter VBGM
414 models have lower annual fecundity and mature later (higher L_{mat}/L_{∞}) than those best
415 described by the Robertson or Gompertz models (Table 7).

416

417 Although VBGM has been widely used in fitting age and length data, where
418 alternative models have not been tried and evaluated, the derived age structure may be
419 biased and inaccurate (Roff, 1980). This will cause further errors in the estimates of
420 mortality, yield per recruit, and stock assessment. If the Robertson or Gompertz
421 models better describe the growth of certain species, variations in different life stages
422 can be considered, and stock assessment will be improved (Carlson & Baremore,
423 2005).

424

425 CONCLUSION

426 The best growth model for elasmobranchs depends on their size and life history
427 characteristics (Fig. 7). VBGM provides the best fit for large pelagic sharks that are
428 late-maturing and of moderate longevity. These include the pelagic thresher and blue
429 sharks. The two-parameter VBGM best fits large pelagic sharks that are slow-growing
430 and have extended longevity, such as the silky and sandbar sharks. The Robertson
431 model is the best fit for fast-growing small sharks that inhabit deep water. For small
432 sharks in shallow waters, the two-parameter VBGM and the Robertson model provide
433 the best description. The Robertson model is also the best fit for medium and small-
434 size demersal skates and rays, which are fast-growing and of short longevity, such as
435 the smooth dogfish and thorny skate. The Gompertz model best fits large or small,

436 median-growing skates and rays, such as the yellow and Kwangtung skates. For the
437 whale shark, with its huge size, slow growth, extended longevity, late maturity, and
438 prolonged reproductive cycle, the two-parameter VBGM provides the best fit.
439

440 **REFERENCES**

- 441 Akaike, H., 1973. Information theory as an extension of the maximum likelihood
442 principle. pp. 267-281. In: Petrov, B.N. and Csaki, F. (eds.) Second international
443 symposium on information theory, Akademiai Kiado, Budapest, Hungary.
444
- 445 Araya, M., Cubillos, L.A., 2006. Evidence of two-phase growth in elasmobranches.
446 Environ. Biol. Fishes 77, 293-300.
447
- 448 Beverton, R.J.H., Holt, S.J., 1957. On the dynamics of exploited fish populations.
449 Fisheries Investment Series 2, Vol. 19, 533 pp. UK Ministry of Agriculture and
450 Fisheries, London.
451
- 452 Braccini J.M., Gillanders, B.M., Walker, T.I., Tovar-Avila, J., 2007. Comparison of
453 deterministic growth models fitted to length-at-age data of the piked spurdog (*Squalus*
454 *megalops*) in south-eastern Australia. Mar. Freshw. Res. 58, 24-33.
455
- 456 Branstetter, S. Musick, J.A., 1994. Age and growth estimates for the sand tiger in the
457 northwestern Atlantic ocean. Trans. Am. Fish. Soc. 123, 242-254.
458
- 459 Burnham, K.P., Anderson D.R., 2002. Model Selection and multimodel inference: A
460 practical-theoretic approach. Springer, New York, 488 pp.
461
- 462 Cailliet, G.M., Goldman, K.J., 2004. Age determination and validation in
463 chondrichthyan fishes. pp. 399-447. In: Carrier, J., Musick, J.A., Heithaus, M.R. (eds.)
464 Biology of sharks and their relatives, CRC Press LLC, Boca Raton, Fla.
465
- 466 Cailliet, G.M., Radtke, M.S., Welden, B.A., 1986. Elasmobranch age determination
467 and verification: a review. pp. 345-359. In: Uyeno, T., Arai, R., Matsuura, T. (eds.)
468 Indo-Pacific Fishes Biology: Proceedings of the Second International Conference on
469 Indo-Pacific Fishes, Ichthyological Society of Japan, Tokyo.
470
- 471 Cailliet, G.M., Smith, W.D., Mollet, H.F., Goldman, K.J., 2006. Age and growth
472 studies and growth of chondrichthyan fishes: the need for consistency in terminology,
473 verification, validation, growth function. Environ. Biol. Fishes 77, 211-228.

474

475 Carlson, J.K., Baremore, I.E., 2003. Changes in biological parameters of Atlantic
476 sharpnose shark *Rhizoprionodon terraenovae* in the Gulf of Mexico: evidence for
477 density-dependent growth and maturity. *Mar. Freshwat. Res.* 54:227-234.

478

479 Carlson, J.K., Baremore, I.E., 2005. Growth dynamics of the spinner shark
480 (*Carcharhinus brevipinna*) off the United States southeast and Gulf of Mexico coasts:
481 a comparison of methods. *Fish. Bull.* 103, 280-291.

482

483 Carlson, J.K., Cortés, E., Bethea, D.M., 2003. Life history and population dynamics
484 of the finetooth shark (*Carcharhinus isodon*) in the northeastern Gulf of Mexico. *Fish.*
485 *Bull.* 101, 281-292.

486

487 Carlson, J.K., Cortés, E. Johnson, A.G., 1999. Age and growth of the blacknose shark,
488 *Carcharhinus acronotus*, in the eastern Gulf of Mexico. *Copeia* 1999, 684-691.

489

490 Carlson, J.K., Parsons, G.R., 1997. Age and growth of the bonnethead shark, *Sphyrna*
491 *tiburo*, from northwest Florida, with comments on clinal variation. *Environ. Biol.*
492 *Fishes* 50, 331-341.

493

494 Chang, J.H., Liu, K.M., 2009. Stock assessment of the shortfin mako shark, *Isurus*
495 *oxyrinchus*, in the Northwest Pacific Ocean using per-recruit and virtual population
496 analyses. *Fish. Res.* 98, 92-101.

497

498 Chen, P., 2004. Comparison of fitting growth equations on fishes with different body
499 shapes. M. Sc. Thesis, National Taiwan Ocean University.

500

501 Chen, W.K., Chen, P.C., Liu, K.M., Wang, S.B., 2007. Age and growth estimates of
502 the whitespotted bamboo shark, *Chiloscyllium plagiosum*, in the northern waters of
503 Taiwan. *Zool. Stud.* 46(1), 92-102.

504

505 Coelho, R., Erzini, K., 2002. Age and growth of the undulate ray, *Raja undulata*, in
506 the Algarve (southern Portugal). *J. Mar. Biol. Assoc. UK* 82, 987-990.

507

- 508 Coelho, R., Erzini, K., 2007. Population parameters of the smooth lantern shark,
509 *Etmopterus pusillus*, in southern Portugal (NE Atlantic). Fish. Res. 86, 42-57.
510
- 511 Coelho, R., Erzini, K., 2008. Life history of a wide-ranging deepwater lantern shark
512 in the north-east Atlantic, *Etmopterus spinax* (Chondrichthyes: Etmopteridae), with
513 implications for conservation. J. Fish Biol. 73, 1419-1443.
514
- 515 Du Buit, M.H., 1977. Age et croissance de *Raja batis* et de *Raja naevus* en Mer
516 Celtique. Journal du Conseil International pour L'exploration de la Mer 37(3), 261-
517 265.
518
- 519 Duffy, K.A., 1999. Feeding, growth and bioenergetics of the chain dogfish,
520 *Scyliorhinus retifer*. Ph. D. Thesis, University of Rhode Island, Kingston, RI.
521
- 522 Ebert, D.A., Smith, W.D., Haas, D.L., Ainsley, S.M., Cailliet, G.M., 2007. Life history
523 and population dynamics of Alaskan skates: providing essential biological
524 information for effective management of bycatch and target species. North Pacific
525 Research Board Project Final Report 130pp.
526
- 527 Fabens, A.J., 1965. Properties and fitting of the von Bertalanffy growth curve. Growth
528 29, 265-289.
529
- 530 Gelsleichter, J., Piercy, A., Musick, J.A., 1998. Evaluation of copper, iron and lead
531 substitution techniques in elasmobranch age determination. J. Fish Biol. 53, 465-470.
532
- 533 Geraghty, P.T., Mecbeth, W.G., Harry, A.V., Bell, J.E., Yerman, M.N., Williamson,
534 J.E., 2014. Age and growth parameters for three heavily exploited shark species off
535 temperate eastern Australia. ICES J. Mar. Sci. 71(3), 559-573.
536
- 537 Gompertz, B., 1825. On the nature of the function expressive of the law of human
538 mortality and on a new mode of determining life contingencies. Philos. Trans. R. Soc.
539 London 115, 513-585.
540
- 541 Haddon, M., 2001. Modelling and quantitative methods in fisheries. Chapman &

- 542 Hall/CRC, 406 pp.
543
- 544 Hoenig, J.M., Gruber, S.H., 1990. Life history patterns in the elasmobranches:
545 implications for fisheries management. pp. 1-15. In: (Pratt, H.L., Gruber, S.H.,
546 Taniuchi, T. (eds.) Elasmobranchs as Living Resources: Advances in the Biology,
547 Ecology, Systematics, and the Status of the Fisheries. NOAA Technical Report NMFS
548 90.
549
- 550 Hsu, H.H., 2009. Age, growth, and migration of the whale shark, *Rhincodon typus*, in
551 the Northwest Pacific. Ph. D. Thesis, National Taiwan Ocean University.
552
- 553 Huang, J.C., 2006. Age and growth of blue shark, *Prionace glauca* in the
554 northwestern Pacific. M. Sc. Thesis, National Taiwan Ocean University.
555
- 556 Ismen, A., 2003. Age, growth, reproduction and food of common stingray (*Dasyatis*
557 *pastinaca* L., 1758) in İskenderun Bay, the eastern Mediterranean. Fish. Res. 60, 169-
558 176.
559
- 560 Ismen, A., Yığın, C., Ismen, P., 2007. Age, growth, reproductive biology and feed of
561 the common guitarfish (*Rhinobatos rhinobatos* Linnaeus, 1758) in İskenderun Bay,
562 the eastern Mediterranean Sea. Fish. Res. 84, 263-269.
563
- 564 Joung, S.J., Lee, P.H., Liu, K.M., Liao, Y.Y., 2011. Estimates of life history
565 parameters of the sharpnose skate, *Okamejei acutispina*, in the northeastern waters of
566 Taiwan. Fish. Res. 108, 258-267.
567
- 568 Joung, S.J., Chen, J.H., Chin, C.P., Liu, K.M., 2015. Age and growth estimates of the
569 dusky shark, *Carcharhinus obscurus*, in the western North Pacific Ocean. Terr.,
570 Atmos. Oceanic Sci. 26(2): 153-160. doi: 10.3319/TAO.2014.10.15.01(Oc).
571
- 572 Joung, S.J., Chen, C.C., Liu, K.M., Hsieh, T.C., 2015. Age and growth estimate of the
573 Kwangtung skate, *Dipturus kwangtungensis* in the northern waters off Taiwan. J. Mar.
574 Biol. Assoc. U. K. doi: 10.1017/S0025315415001307.
575

- 576 Katsanevakis, S., 2006. Modelling fish growth: Model selection, multi-model
577 inference and model selection uncertainty. *Fish. Res.* 81, 229-235.
578
- 579 Katsanevakis, S., Maravelias, C.D., 2008. Modelling fish growth: multi-model
580 inference as a better alternative to a priori using von Bertalanffy equation. *Fish Fish.* 9,
581 178-187.
582
- 583 King, J.R., McFarlane, G.A., 2003. Marine fish life history strategies: applications to
584 fishery management. *Fish. Manage. Ecol.* 10, 249-264.
585
- 586 Kneebon, J., Nantanson, L.J., Andrews, A.H., Howell, W.H., 2008. Using bomb
587 radiocarbon analyses to validate age and growth estimates for the tiger shark,
588 *Galeocerdo cuvier*, in the western North Atlantic. *Mar. Biol.* 154, 423-434.
589
- 590 Lessa, R., Santana, F.M., 1998. Age determination and growth of the smalltail shark,
591 *Carcharhinus porosus*, from northern Brazil. *Mar. Freshw. Res.* 49, 705-711.
592
- 593 Lessa, R., Santana, F.M., Batists, V., Almeida, Z., 2000. Age and growth of the
594 daggernose shark, *Isogomphodon oxyrinchus*, from northern Brazil. *Mar. Freshw.*
595 *Res.* 51, 339-47.
596
- 597 Lessa, R., Santana, F.M., Hazin, F.H., 2004. Age and growth of the blue shark
598 *Prionace glauca* (Linnaeus, 1758) off northeastern Brazil. *Fish. Res.* 66, 19-30.
599
- 600 Lessa, R., Santana, F.M., Pagleran, i R., 1999. Age, growth and stock structure of the
601 oceanic whitetip shark, *Carcharhinus longimanus*, from the southwestern equatorial
602 Atl. *Fish. Res.* 42, 21-30.
603
- 604 Licandeo, R.R., Lamilla, J.G., Rubilar, P.G., Vega, R.M., 2006. Age, growth, and
605 sexual maturity of the yellownose skate *Dipturus chilensis* in the south-eastern Pacific.
606 *J. Fish Biol.* 68, 488-506.
607
- 608 Liu, K.M., Chen, C.T., Liao, T.H., Joung, S.J., 1999. Age, growth and reproduction of
609 the pelagic thresher shark, *Alopias pelagicus* in the northwestern Pacific. *Copeia* 1,

610 68-74.

611

612 Liu, K.M., Chin, C.P., Chen, C.H., and Chang, J.H., 2015. Estimating finite rate of
613 population increase for sharks based on vital parameters. PloS One doi:

614 10.1371/journal.pone.0143008.

615

616 Loefer, J.K., Sedberry, G.R., 2003. Life history of the Atlantic sharpnose shark
617 (*Rhizoprionodon terraenovae*) (Richardson, 1836) off the southeastern United States.

618 Fish. Bull. 101, 75-88.

619

620 Matta, M.E., Gunderson, D.R., 2007. Age, growth, maturity, and mortality of the
621 Alaska skate, *Bathyraja parmifera*, in the eastern Bering Sea. Environ. Biol. Fishes 80,

622 309-323.

623

624 Mollet, H.F., Ezcurra, J.M., O'Sullivan, J.B., 2002. Captive biology of the pelagic
625 stingray, *Dasyatis violacea* (Bonaparte, 1832). Mar. Freshw. Res. 53, 531-541.

626

627 Moulton, P.L., Walker, T.I., Saddler, S.R., 1992. Age and growth studies of gummy
628 shark, *Mustelus antarcticus* Günther, and school shark, *Galeorhinus galeus*

629 (Linnaeus), from southern Australian waters. Aust. J. Mar. Freshw. Res. 43, 1241-

630 1267.

631

632 Natanson, L.J., Gervelis, B.J., Winton, M.V., Hamady, L.L., Gulak, S.J.B., Carlson,
633 J.K., 2014. Validated age and growth estimates for *Carcharhinus obscurus* in the

634 northwestern Atlantic Ocean, with pre- and post- management growth comparisons.

635 Environ. Biol. Fishes 97, 881-896. doi: 10.1007/s10641-013-0189-4.

636

637 Natanson, L.J., Kohler, N.C., Ardizzone, D., Cailliet, G.M., Wintner, S.P., Mollet,

638 H.F., 2006. Validated age and growth estimates for the shortfin mako, *Isurus*

639 *oxyrinchus*, in the North Atlantic Ocean. Environ. Biol. Fishes 77, 367-383.

640

641 Natanson, L.J., Sulikowski, J.A., Kneebone, J.R., Tsang, P.C., 2007. Age and growth

642 estimates for the smooth skate, *Malacoraja senta*, in the Gulf of Maine. Environ. Biol.

643 Fishes 80, 293-308.

644

645 Natanson, L.J., Gervelis B.J., Winton, M.V., Hamady L.L., Gulak, S.J.B., Carlson,
646 J.K., 2014. Validated age and growth estimates for *Carcharhinus obscurus* in the
647 northwestern Atlantic Ocean, with pre- and post management growth comparisons.
648 Environ. Biol. Fishes 97(8), 881-896.

649

650 Neer, J.A., Cailliet, G.M., 2001. Aspects of the life history of the Pacific electric ray,
651 *Torpedo californica* (Ayres). Copeia 2001, 842-847.

652

653 Neer, J.A., Thompson, B.A., Carlson, J.K., 2005. Age and growth of *Carcharhinus*
654 *leucas* in the northern Gulf of Mexico: incorporating variability in size at birth. J. Fish
655 Biol. 67, 370-383.

656

657 Oshitani, S., Nakano, H., Tanaka, S., 2003. Age and growth of the silky shark
658 *Carcharhinus falciformis* from the Pacific Ocean. Fish. Sci. 69, 456-464.

659

660 Piercy, A.N., Carlson, J.K., Sulikowski, J.A., Burgess, G.H., 2007. Age and growth of
661 the scalloped hammerhead shark, *Sphyrna lewini*, in the north-west Atlantic Ocean
662 and Gulf of Mexico. Mar. Freshw. Res. 58, 34-40.

663

664 Pütter, A., 1920. Studien über physiologische Ähnlichkeit VI.
665 Wachstumsähnlichkeiten. Pflugers Arch. Gesamte Physiol. Menschen Tiere 180, 298-
666 340.

667

668 Quinn II, T.J., Deriso, R.B., 1999. Quantitative Fish Dynamics. 542 pp. New York:
669 Oxford University Press.

670

671 Ricker, W.E., 1975. Computation and interpretation of biological statistics of fish
672 populations. J. Fish. Res. Board Can. 191, 1-382.

673

674 Ricker, W.E., 1979. Growth rate and models. Fish Physiology VIII series, 677-743.
675 San Diego, CA: Academic Press.

676

677 Robertson, T.B., 1923. The chemical basis of growth and senescence. J.B. Lippincott,

- 678 Philadelphia & London, 389 pp.
679
- 680 Roff, D.A., 1980. A motion for the retirement of the von Bertalanffy function. Can. J.
681 Fish. Aquat. Sci. 37, 127-129.
682
- 683 Romine, J.G., Grubbs, R.D., Musick, J.A., 2006. Age and growth of the sandbar shark,
684 *Carcharhinus plumbeus*, in Hawaiian waters through vertebral analysis. Environ. Biol.
685 Fishes 77, 229-239.
686
- 687 Romney, P.M., Campana, S.E., 2009. Bomb dating and age determination of skates
688 (family Rajidae) off the eastern coast of Canada. J. Mar. Sci. 66, 546-560.
689
- 690 Santana, F.M., Lessa, R., 2004. Age determination and growth of the night shark
691 (*Carcharhinus signatus*) off the northeastern Brazilian coast. Fish. Bull. 102, 156-167.
692
- 693 Schmid, T.H., Murru, F.L., 1994. Bioenergetics of the bull shark, *Carcharhinus leucas*,
694 maintained in captivity. Zool. Biol. 13, 177-185.
695
- 696 Semba, Y., Nakano, H., and Aoki, I., 2009. Age and growth analysis of the shortfin
697 mako, *Isurus oxyrinchus*, in the western and central North Pacific Ocean. Environ.
698 Biol. Fishes 84, 377-391. doi: 10.1007/s10641-009-9447-x.
699
- 700 Simpfendorfer, C.A., Cdlow, J., McAuley, R., Unsworth, P., 2000. Age and growth of
701 the whiskery shark, *Furgaleus macki*, from southwestern Australia. Environ. Biol.
702 Fishes 58, 335-343.
703
- 704 Simpfendorfer, C.A., McAuley, R.B., Chidlow J., Unsworth P., 2002. Validated age
705 and growth of the dusky shark, *Carcharhinus obscurus*, from Western Australian
706 waters. Mar. Freshw. Res. 53, 567-573.
707
- 708 Soriano, M., Moreau, J., Hoenig, J.M. & Pauly, D., 1992. New functions for the
709 analysis of two-phase growth of juvenile and adult fishes, with application to Nile
710 perch. Trans. Am. Fish. Soc. 121, 486-493.
711

- 712 Stevens, J.D., Bonfil, R., Dulvy, N.K. & Walker, P.A., 2000. The effects of fishing on
713 sharks, rays, and chimaeras (chondrichthyans), and the implications for marine
714 ecosystems. *ICES J. Mar. Sci.* 57, 476-494.
715
- 716 Sulikowski, J.A., Irvine, S.B., DeValerio, K.C., Carlson, J.K., 2007. Age, growth and
717 maturity of the roundel skate, *Raja texana*, from the Gulf of Mexico, USA. *Mar.*
718 *Freshw. Res.* 58, 41-53.
719
- 720 Sulikowski, J.A., Kneebone, J., Elzey, S., 2005. Age and growth estimates of the
721 thorny skate (*Amblyraja radiata*) in the western Gulf of Maine. *Fish. Bull.* 103, 161-
722 168.
723
- 724 Sulikowski, J.A., Morin, M.D., Suk, S.H., Howell, W.H., 2003. Age and growth
725 estimates of the winter skate (*Leucoraja ocellata*) in the western Gulf of Maine. *Fish.*
726 *Bull.* 101, 405-413.
727
- 728 Thorson, J.T., Simpfendorfer, C.A., 2009. Gear selectivity and sample size effects on
729 growth curve selection in shark age and growth studies. *Fish. Res.* 98, 75-84.
730
- 731 von Bertalanffy, L., 1938. A quantitative theory of organic growth (Inquires on growth
732 laws II). *Hu. Biol.* 10, 181-213.
733
- 734 Wang, T.M., Chen, C.T., 1982. Age and growth of smooth dogfish, *Mustelus griseus*,
735 in northwestern Taiwan waters. *J. Fish. Soc. Taiwan* 9, 1-12.
736
- 737 Wang, Z., Zuidhof, M.J., 2004. Estimation of growth parameters using a nonlinear
738 mixed Gompertz model. *Poul. Sci.* 83, 847-852.
739
- 740 Waring, G.T., 1984. Age, growth, and mortality of the little skate off the northeast
741 coast of the United States. *Trans. Am. Fish. Soc.* 113, 314-321.
742
- 743 Winberg, G. G. (1960). Rate of metabolism and food requirements of fishes. *Fish. Res.*
744 *Board Can.* 194, 1-202.
745

- 746 Winemiller, K.O., Rose, K.A., 1992. Patterns of life-history diversification in north
747 American fishes: implication for population regulation. *Can. J. Fish. Aquat. Sci.* 49,
748 2196-2218.
749
- 750 Winsor, C.P., 1932. The Gompertz curve as a growth curve. *Natl. Acad. Sci.* 18(1), 1-
751 8.
752
- 753 Wintner, S.P., Cliff, G., 1996. Age and growth determination of the blacktip shark,
754 *Carcharhinus limbatus*, from the east coast of South Africa. *Fish. Bull.* 94, 135-144.
755
- 756 Wintner, S.P., Dudley, S.F.J., 2000. Age and growth estimates for the tiger shark,
757 *Galeocerdo cuvier*, from the east coast of South Africa. *Mar. Freshw. Res.* 51, 43-53.
758
- 759 Wintner, S.P., Dudley, S.F.J., Kistnasamy, N., Everett, B., 2002. Age and growth
760 estimates for the Zambezi shark, *Carcharhinus leucas*, from the east coast of South
761 Africa. *Mar. Freshw. Res.* 53, 557-566.
762

763 Table 1

764 Age-length data, reproduction strategy and the information of age determination used

765 in the present study

766

Sample No.	Scientific name	Sample Size	Data		R	Precision	Verification	Ageing	References
			source	Length					
1	<i>Amblyraja radiata</i>	224	a	TL	o	CV	MIR	Ver	Sulikowski et al., 2005*
2	<i>Carcharhinus acronotus</i>	67	a	FL	v	IAPE	MIR	Ver	Carlson et al., 1999*
3	<i>C. brevipinna</i>	258	a	FL	v	IAPE	MIR	Ver	Carlson & Baremore, 2005
4	<i>C. falciformis</i>	289	a	PCL	v	-	MIR	Ver	Oshitani et al., 2003
5	<i>C. isodon</i>	240	a	TL	v	-	MIR	Ver	Carlson et al., 2003
6	<i>C. leucas</i>	117	a	PCL	v	IAPE	MIR	Ver	Wintner et al., 2002
7	<i>C. longimanus</i>	107	a	TL	v	IAPE	MIR	Ver	Lessa et al., 1999
8	<i>C. plumbeus</i>	186	a	PCL	v	IAPE	MIR	Ver	Romine et al., 2006
9	<i>C. porosus</i>	504	a	TL	v	IAPE	MIR	Ver	Lessa & Santana, 1998
10	<i>Dasyatis pastinaca</i>	49	a	TL	ov	IAPE	MIR	Ver	Ismen, 2003
11	<i>Dipturus chilensis</i>	400	a	TL	o	IAPE	MIR	Ver	Licandeo et al., 2006*
12	<i>Etmopterus pusillus</i>	523	a	TL	ov	IAPE, CV	MIR	Sp	Coelho & Erzini, 2007
13	<i>Etmopterus spinax</i>	733	a	TL	ov	IAPE, CV	MIR	Sp	Coelho & Erzini, 2008
14	<i>Galeocerdo cuvier</i>	90	a	PCL	v	IAPE	MIR	Ver	Wintner & Dudley, 2000*
15	<i>Isogomphodon oxyrinchus</i>	105	a	TL	ov	IAPE	MIR	Ver	Lessa et al., 2000*
16	<i>Leucoraja ocellata</i>	209	a	TL	o	IAPE	MIR	Ver	Sulikowski et al., 2003
17	<i>Odontaspis taurus</i>	52	a	TL	v	-	MIR	Ver	Branstetter & Mustck, 1994
18	<i>Raja texana</i>	231	a	TL	o	IAPE	MIR	Ver	Sulikowski et al., 2007*
19	<i>Rhizoprionodon terraenovae</i>	804	a	PCL	v	IAPE	MIR	Ver	Loefer & Sedberry, 2003
20	<i>Sphyrna lewini</i>	307	a	FL	v	IAPE	MIR	Ver	Piercy et al., 2007
21	<i>Mustelus griseus</i>	207	a	TL	v	IAPE	MIR	Ver	Wang & Chen, 1982*
22	<i>Carcharhinus limbatus</i>	92	a	PCL	v	IAPE	MIR	Ver	Wintner & Cliff, 1996
23	<i>Rhinobatos rhinobatos</i>	80	a	TL	o	IAPE	MIR	Ver	Ismen et al., 2007
24	<i>Galeorhinus galeus</i>	395	b	TL	ov	IAPE	MIR	Ver	Moulton et al., 1992*
25	<i>M. antarcticus</i>	516	b	TL	ov	IAPE	MIR	Ver	Moulton et al., 1992*
26	<i>Raja batias</i>	81	b	TL	o	IAPE	MIR	Ver	Du Buit, 1977*
27	<i>R. naevus</i>	48	b	TL	o	IAPE	MIR	Ver	Du Buit, 1977
28	<i>R. erinaceian</i>	777	b	TL	o	IAPE	MIR	Ver	Waring, 1984*
29	<i>R. undulata</i>	182	b	TL	o	-	MIR	Ver	Coelho & Erzini, 2002
30	<i>Carcharhinus signatus</i>	317	b	TL	v	IAPE	MIR	Ver	Santana & Lessa, 2004*
31	<i>Alopias pelagicus</i>	269	c	PCL	v	-	MIR	Ver	Liu et al., 1999*
32	<i>D. kwangtungensis</i>	394	c	TL	o	-	MIR	Ver	Joung et al., 2015*
33	<i>P. glauca</i>	431	c	TL	v	IAPE	MIR	Ver	Huang, 2006*
34	<i>Okamejei acutispina</i>	329	c	DW	o	-	MIR	Ver	Joung et al., 2011
35	<i>Chiloscyllium plagiosum</i>	429	c	TL	o	IAPE, PA	MIR	Ver	Chen et al., 2007
36	<i>C. obscurus</i>	387	c	TL	v	-	MIR	Ver	Joung et al., 2015*
37	<i>Rhincodon typus</i>	84	c	TL	ov	-	MIR	Ver	Hsu, 2009

767

768 “a” : sample simulation, “b” : age-length-key, “c” : original data, “Ver” : vertebrae,

769 “Sp” : spines, * : no L₀, “R” : reproduction strategy, “o” : oviparity, “v” : viviparity,

770 “ov” : aplacental viviparity, “CV” : coefficient of variation, “PA” : percent agreement,

771 “IAPE” : index of average percentage error, “MIR” : marginal increment ratio

772 analysis.

773

774 Table 2

775 A list of elasmobranches used in the present study

776

Order	Family	Scientific name	Common name	
Orectolobiformes	Hemiscylliidae	<i>Chiloscyllium plagiosum</i>	Whitespotted Bamboo Shark	
	Rhincodontidae	<i>Rhincodon typus</i>	Whale shark	
Lamniformes	Odontaspidae	<i>Odontaspis taurus</i>	Sand tiger shark	
	Alopiidae	<i>Alopias pelagicus</i>	Pelagic thresher shark	
Carcharhiniformes	Triakidae	<i>Galeorhinus galeus</i>	School shark	
		<i>Mustelus antarcticus</i>	Gummy shark	
		<i>M. griseus</i>	Smooth dogfish	
	Carcharhinidae	<i>Carcharhinus acronotus</i>	Blacknose shark	
		<i>C. brevipinna</i>	Spinner shark	
		<i>C. falciformis</i>	Silky shark	
		<i>C. isodon</i>	Finetooth shark	
		<i>C. leucas</i>	Bull Shark	
		<i>C. limbatus</i>	Blacktip shark	
		<i>C. longimanus</i>	Oceanic whitetip shark	
		<i>C. obscurus</i>	Dusky shark	
		<i>C. plumbeus</i>	Sandbar shark	
		<i>C. porosus</i>	Smalltail shark	
		<i>C. signatus</i>	Night shark	
		<i>Galeocerdo cuvier</i>	Tiger shark	
		<i>Isogomphodon oxyrhynchus</i>	Daggernose shark	
		<i>Prionace glauca</i>	Blue shark	
		<i>Rhizoprionodon terraenovae</i>	Atlantic sharpnose shark	
		Sphyrnidae	<i>Sphyrna lewini</i>	Scalloped hammerhead shark
		Squaliformes	Etmopteridae	<i>Etmopterus pusillus</i>
<i>E. spinax</i>	Deepwater lantern shark			
Rajiformes	Rhinobatidae	<i>Rhinobatos rhinobatos</i>	Common guitarfish	
	Rajidae	<i>Amblyraja radiata</i>	Thorny skate	
		<i>Leucoraja ocellata</i>	Winter skate	
		<i>Raja batis</i>	Blue skate	
		<i>R. erinaceian</i>	Little skate	
		<i>D. kwangtungensis</i>	Kwangtung skate	
		<i>R. naevus</i>	Cuckoo ray	
		<i>R. texana</i>	Roundel skate	
		<i>R. undulata</i>	Undulate ray	
<i>Okamejei acutispina</i>	Sharpspine skate			
Myliobatiformes	Dasyatidae	<i>Dasyatis pastinaca</i>	Common stingray	

777

778

779 Table 3

780 Growth parameters of the species best fitted by VBGM. Parenthese indicate

781 standard errors.

Scientific name	Common name	L_{∞} (cm)	k (yr ⁻¹)	t_0
<i>Galeocerdo cuvier</i>	Tiger shark	364.3 (48.62)	0.1181 (0.0360)	-2.300 (0.6808)
<i>Raja texana</i>	Roundel skate	66.8 (4.84)	0.1944 (0.0449)	-1.071 (0.5341)
<i>Raja batis</i>	Blue skate	47.6 (8.31)	0.0240 (0.0055)	-2.502 (0.3027)
<i>Carcharhinus signatus</i>	Night shark	303.9 (23.12)	0.0746 (0.0132)	-4.947 (0.6565)
<i>Alopias pelagicus</i>	Pelagic thresher shark	189.5 (7.25)	0.1001 (0.0152)	-6.469 (0.9374)
<i>Prionace glauca</i>	Blue shark	355.8 (7.84)	0.1328 (0.0081)	-1.522 (0.1819)

782 L_{∞} : asymptotic length, k: growth coefficient, t_0 : theoretical age at zero length.

783

784 Table 4

785 Growth parameters of the species best fitted by the two-parameter VBGM.

786 Parenthese indiccate standard errors.

Scientific name	Common name	L_{∞} (cm)	k (yr ⁻¹)	L_0
<i>Carcharhinus falciformis</i>	Silky shark	315.2 (10.16)	0.0732 (0.0035)	56.1
<i>Carcharhinus isodon</i>	Finetooth shark	144.46 (31.25)	0.3015 (0.0221)	64.2
<i>Carcharhinus leucas</i>	Bull shark	255.9 (4.61)	0.1407 (0.0099)	47.0
<i>Carcharhinus longimanus</i>	Oceanic whitetip shark	271.2 (13.80)	0.1114 (0.0124)	82.0
<i>Carcharhinus plumbeus</i>	Sandbar shark	160.2 (4.41)	0.0815 (0.0057)	52.1
<i>Etmopterus pusillus</i>	Smooth lantern shark	53.1 (0.69)	0.1365 (0.0043)	16.3
<i>Odontaspis Taurus</i>	Sand tiger shark	299.5 (9.79)	0.1782 (0.0161)	100.0
<i>Rhizoprionodon terraenovae</i>	Atlantic sharpnose shark	74.9 (4.41)	0.5815 (0.0210)	32.1
<i>Sphyrna lewini</i>	Scalloped hammerhead shark	219.9 (4.11)	0.1198 (0.0063)	41.1
<i>Carcharhinus limbatus</i>	Blacktip shark	193.6 (7.01)	0.2084 (0.0206)	41.0
<i>Rhinobatos rhinobatos</i>	Common guitarfish	153.6 (29.39)	0.2058 (0.0636)	31.0
<i>Mustelus antarcticus</i>	Gummy shark	206.2 (11.22)	0.0715 (0.0070)	63.7
<i>Raja naevus</i>	Cuckoo ray	95.1 (6.02)	0.0996 (0.0112)	14.5
<i>Raja undulata</i>	Undulate ray	110.1 (4.25)	0.1049 (0.0074)	21.6
<i>Chiloscyllium plagiosum</i>	Whitespotted bamboo shark	106.3 (4.57)	0.1721 (0.0131)	15.0
<i>Rhincodon typus</i>	Whale shark	158.0 (30.49)	0.0197 (0.0048)	57.9

787 L_{∞} : asymptotic length, k: growth coefficient, L_0 : size at birth.

788

789 Table 5

790 Growth parameters of the species best fitted by the Robertson model. Parenthese

791 indicate standard errors.

Scientific name	Common name	L_{∞} (cm)	k_r (yr ⁻¹)	c_r
<i>Amblyraja radiata</i>	Thorny skate	110.2 (1.96)	0.2664 (0.0113)	1.521 (0.0418)
<i>Carcharhinus acronotus</i>	Blacknose shark	104.8 (4.13)	0.6302 (0.0917)	0.764 (0.0926)
<i>Carcharhinus brevipinna</i>	Spinner shark	188.4 (4.70)	0.2415 (0.0122)	0.735 (0.0607)
<i>Carcharhinus porosus</i>	Smalltail shark	98.9 (1.54)	0.3113 (0.0105)	0.706 (0.0317)
<i>Dasyatis pastinaca</i>	Common stingray	93.4 (3.50)	0.3158 (0.0171)	1.272 (0.0880)
<i>Etmopterus spinax</i>	Deepwater lantern shark	42.3 (0.58)	0.3730 (0.0097)	0.885 (0.0314)
<i>Isogomphodon oxyrinchus</i>	Daggernose shark	151.2 (5.22)	0.2803 (0.0242)	0.664 (0.0638)
<i>Mustelus griseus</i>	Smooth dogfish	90.4 (2.13)	0.3518 (0.0248)	0.699 (0.0406)
<i>Galeorhinus galeus</i>	School shark	159.8 (3.26)	0.2567 (0.0201)	0.579 (0.0389)
<i>Raja erinaceian</i>	Little skate	49.5 (0.35)	0.6665 (0.0215)	0.930 (0.0211)
<i>Okamejei acutispina</i>	Sharpspine skate	31.7 (1.00)	0.3343 (0.0301)	1.290 (0.0615)
<i>Carcharhinus obscurus</i>	dusky shark	362.9 (8.56)	0.1306 (0.0079)	0.911 (0.0462)

792 L_{∞} : asymptotic length, k_r : growth coefficient of Robertson model, c_r : Roberson

793 parameter.

794

795 Table 6

796 Growth parameters of the species best fitted by the Gompertz model. Parenthese

797 indicate standard errors.

Scientific name	Common name	L_{∞} (cm)	k_g (yr ⁻¹)	c_g
<i>Dipturus chilensis</i>	Yellownose skate	113.9 (2.12)	0.1915 (0.0136)	0.581 (0.0336)
<i>Leucoraja ocellata</i>	Winter skate	102.1 (1.61)	0.1531 (0.0048)	0.592 (0.0162)
<i>Dipturus kwangtungensis</i>	Kwangtung skate	96.7 (16.18)	0.1138 (0.0195)	0.621 (0.1729)

798 L_{∞} : asymptotic length, k_g : growth coefficient of Gompertz model, c_g : Gompertz

799 parameter.

800

801 Table 7

802 The parameters of maturity and reproduction of elasmobranches in each best model

803

Scientific name	Model	L_{mat}	L_{mat}/L_{∞}	f	R_c	f/R_c	References
<i>Alopias pelagicus</i>	V	287.00	0.78	2.00	1.00	2.00	Liu et al., 1999
<i>C. brevipinna</i>	R	222.50	0.83	8.50	2.00	4.25	Carlson & Baremore, 2005
<i>C. limbatus</i>	V_2	212.37	0.81	8.00	2.00	4.00	Wintner & Cliff, 1996
<i>Dasyatis pastinaca</i>	R	46.00	0.49	5.50	1.00*	5.50	Ismen, 2003
<i>Okamejei acutispina</i>	R	26.23	0.56	9.00	1.00*	9.00	Joung et al., 2011
<i>Raja batis</i>	V	130.75	0.50	40.00	1.00*	40.00	Du Buit, 1977
<i>R. naevus</i>	V_2	47.00	0.62	102.00	1.00	102.00	Du Buit, 1977

804

805 V: VBGM, V_2 : two-parameter VBGM, R: Robertson model, G: Gompertz806 model, L_{mat} : size at maturity, L_{mat}/L_{∞} : ratio of size at maturity and807 asymptotic length, f: fecundity, R_c : reproductive cycle, f/R_c : annual

808 fecundity.*: Reproductive cycle is assumed to be 1 year

809

810 **Figure legend**

811 Fig 1

812 The percentage of four growth models being selected as the best model, categorized
813 by sharks, skates and rays.

814 Fig 2

815 The percentage of large sharks, small sharks and skates and rays in each best fit
816 growth model.

817 Fig 3

818 The percentage of best growth model for each group.

819 Fig 4

820 The relationship between asymptotic length estimated from each growth model and
821 averaged asymptotic length.

822 Fig 5

823 The second-best choice for each best growth model.

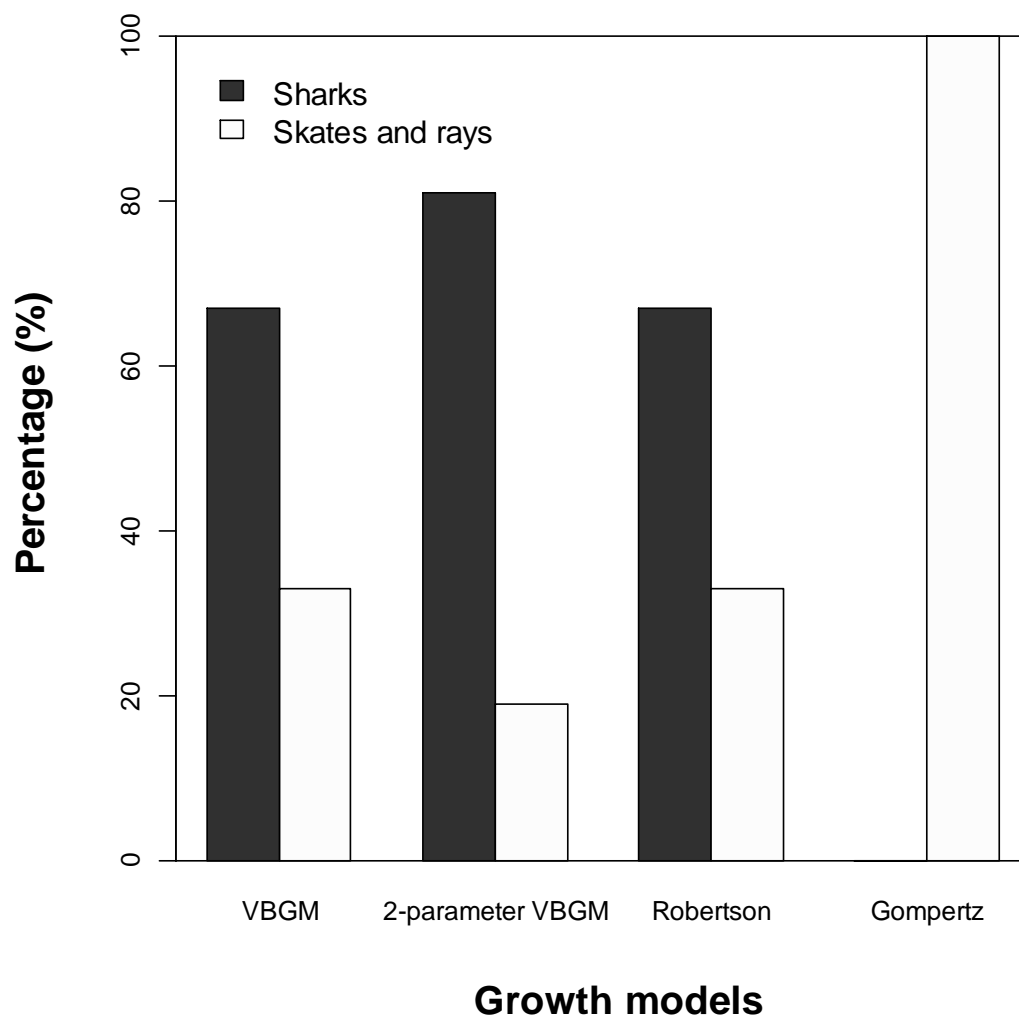
824 Fig 6

825 The percentage of reproduction types for each best growth model.

826 Fig 7

827 The flow chart of selecting the best growth model for elasmobranches.

828

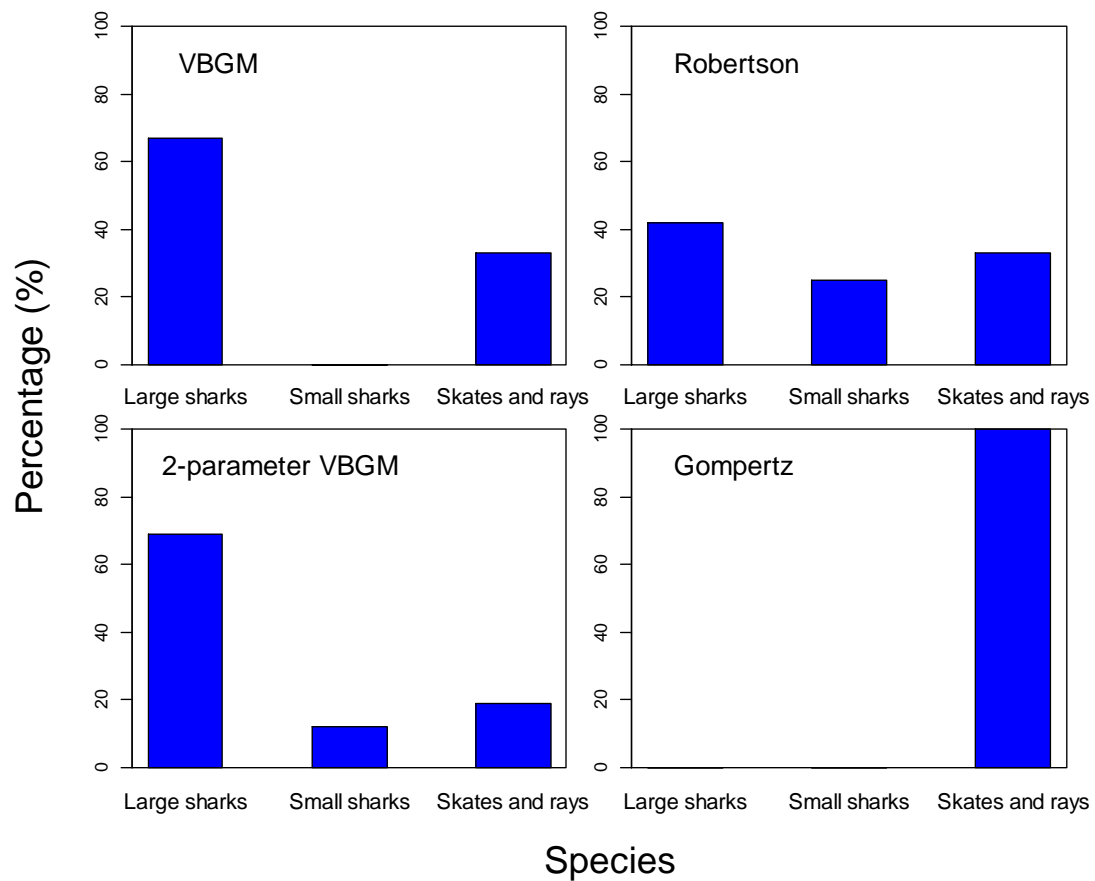


829

830 Figure 1 The percentage of four growth models being selected as the best model,
831 categorized by sharks, skates and rays.

832

833

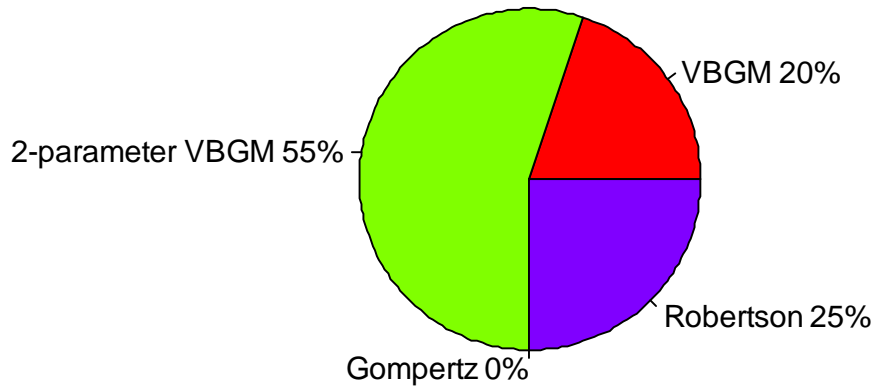


834

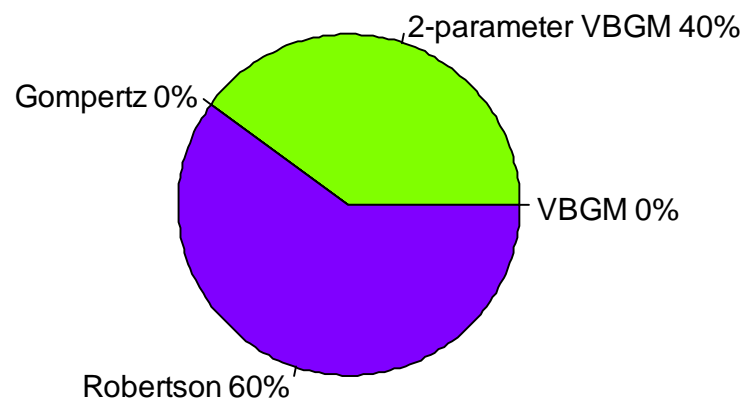
835 Figure 2 The percentage of large sharks, small sharks and skates and rays in each best
836 fit growth model.

837

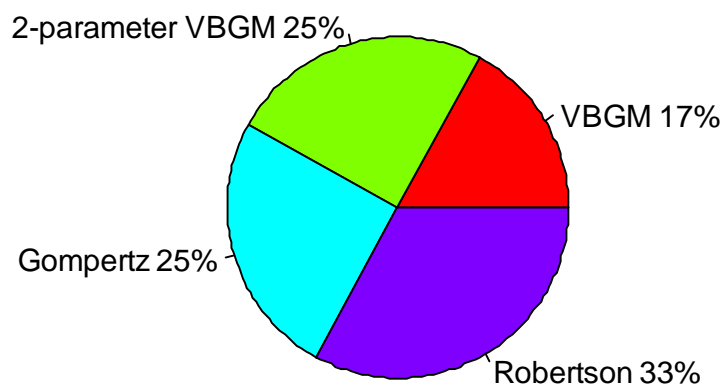
Large sharks



Small sharks



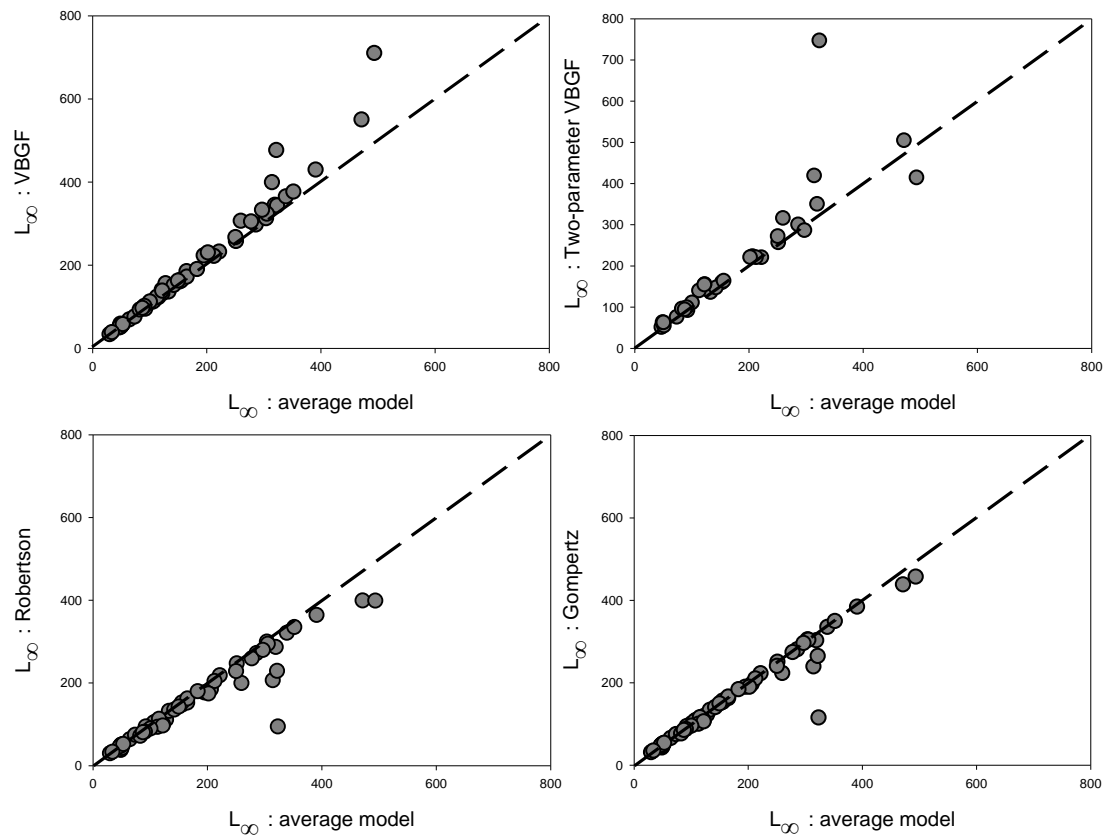
Skates and rays



838

839 Figure 3 The percentage of best growth model for each group.

840



841
842

843 Figure 4 The relationship between asymptotic length estimated from each growth
844 model and averaged asymptotic length.

845

846

847

848

849

850

851

852

853

854

855

856

857

858

859

860

861

862

863

864

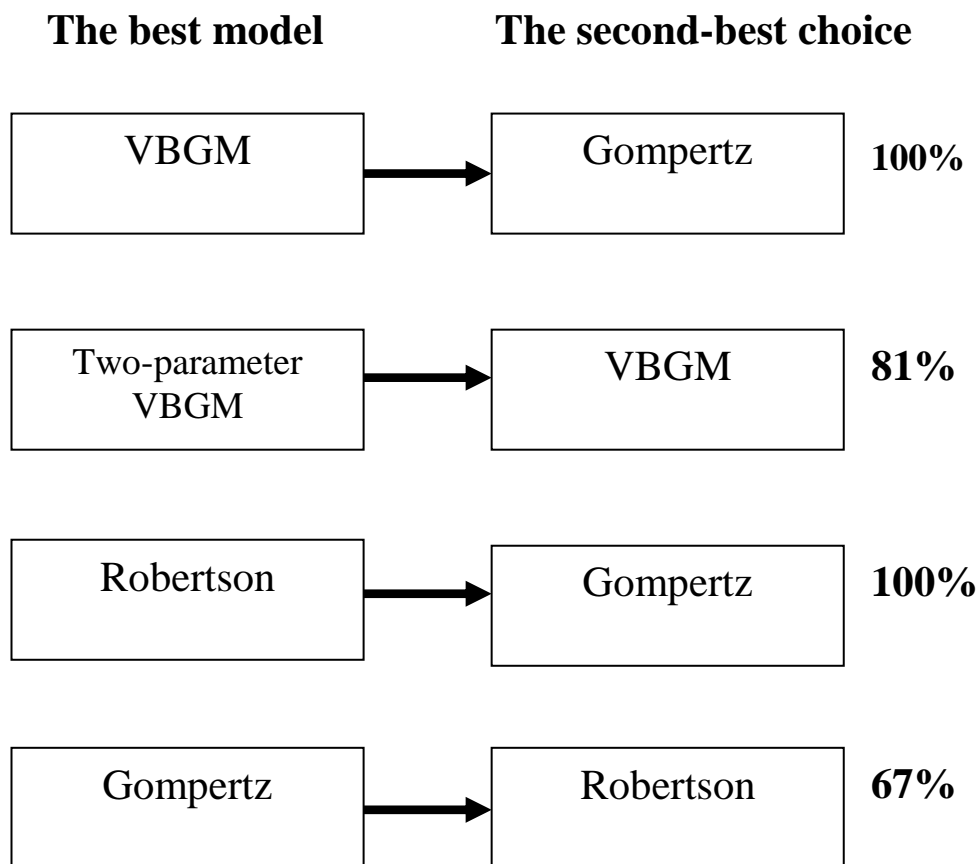
865

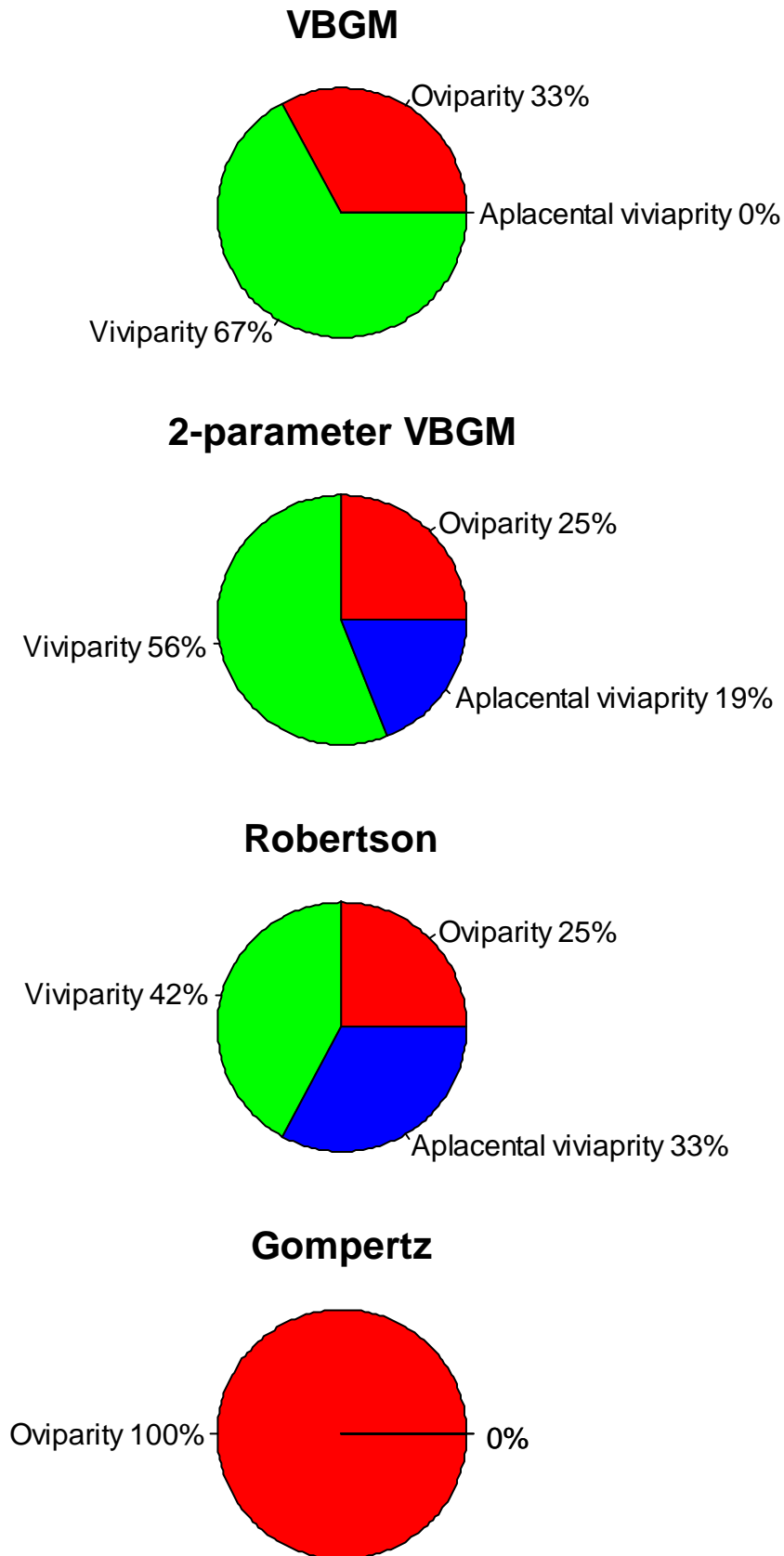
866

867 Figure 5 The second-best choice for each best growth model.

868

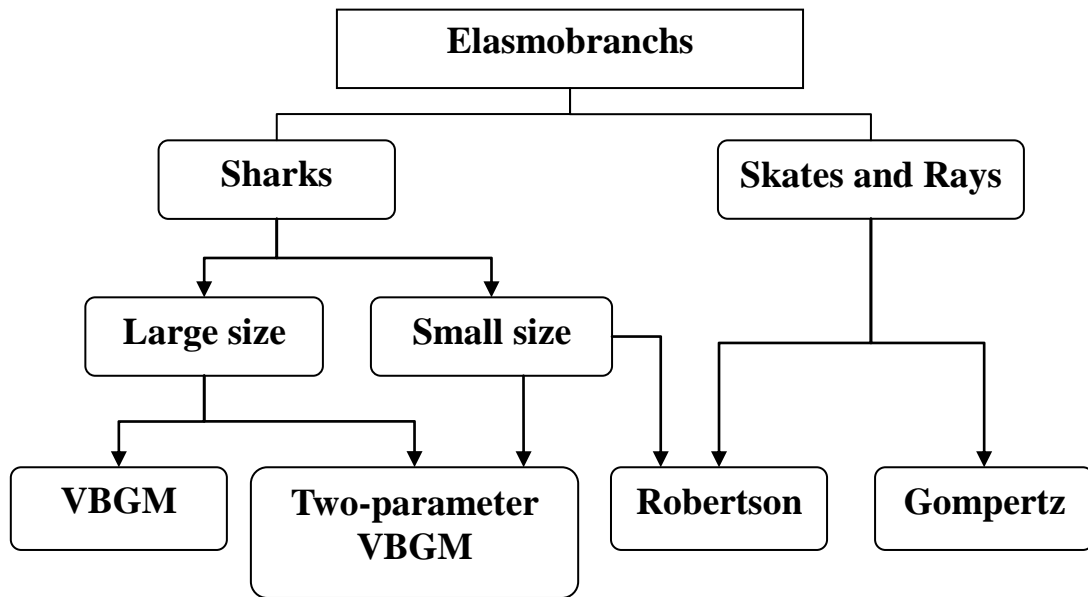
869





870

871 Figure 6 The percentage of reproduction types for each best growth model.



884

885 Figure 7 The flow chart of selecting the best growth model for elasmobranchs.

886